Predictive Model and Deterministic Mechanism in a Bubbling Fluidized Bed

Gui-Bing Zhao, Ji-Zhong Chen, and Yong-Rong Yang
Chemical Engineering Dept., Zhejiang University, Hangzhou 310027, P.R. China

A predictive model based on the theory of phase space reconstruction was proposed to study the determinism and predictability of dynamics underlying pressure fluctuations by measuring and analyzing the time series of pressure signals at different locations in a bubble bed with 0.3 m in dia. and 3 m in height. Chaotic invariants (correlation dimension, K_2 entropy, and Lyapunov exponent spectrum) of measured and model-generated time series of pressure signals were nearly the same. The model captured some important nonlinear characteristics of the real system, which can be used to study the dynamics of fluidizing system. Deterministic dynamics underlying pressure signals were confirmed to exist. A new characteristic index defined as the determining level of dynamics was used to analyze deterministic degrees at different gas velocities and locations of the wall in the bed. Since prediction errors of pressure fluctuations grow exponentially with time at short time scales and the exponent separation rate between predicted and measured values is proportional to the maximal Lyapunov exponent, the long-term predictability of pressure fluctuations is impossible. This verified chaotic properties of fluctuation dynamics in the fluidized bed with deterministic mechanism and sensitive dependence on initial conditions.

Introduction

Pressure fluctuations in fluidized beds have been extensively studied. A great advantage of the study of pressure signals is that they include the effects of many different (dynamical) phenomena taking place in fluidized beds, such as gas turbulence, bubble formation, passage and eruption of bubbles, self-excited oscillations of fluidized particles, pressure oscillations in the plenum chamber due to piston-like motion of the bed, and bubble coalescence and splitting (Bi et al., 1995; Van der Schaaf et al., 1998). Just because pressure fluctuations in fluidized beds contain much rich information (like a "fingerprint" of the global hydrodynamic behavior of the bed), the invariant properties of the time series of pressure fluctuations by analyzing in different ways can be used to characterize flow regime transitions (Yerushalmi and Cankurt, 1979; Lee and Kim, 1988; Brereton and Grace, 1992; Zijerveld et al., 1998; Bai et al., 1999) and index the quality of fluidization (see Schouten and van den Bleek (1998) for a review on monitoring and control of the dynamical state of the fluidized bed).

The nature of pressure fluctuations in a fluidized bed is a complex function of particle properties, bed geometry, pressure in the bed, and properties and flow condition of the fluidizing fluid. Therefore, the study of the essence of pressure fluctuations in fluidized beds is very helpful for intensively understanding the complex hydrodynamical behavior of fluidized beds. In principle, three types of fluctuation essence pressure signals have been presented in literature: (1) periodic fluctuation; (2) random fluctuation; (3) chaos. Verloop and Heertjes (1974) reported that harmonic oscillations of the pressure around its equilibrium value would occur when bed heights are not larger than the critical height of a few hundred particle diameters. Therefore, purely periodic pressure fluctuations would appear and the frequency is proportional to $L^{-0.5}$. For bed heights larger than the critical height, the fluctuations cease to be harmonic, the bed breaks up, and voids are formed leading to the formation of bubbles or slugs; thus, pressure fluctuations become the rather irregular vibrations. The presence of a periodic component in the pressure fluctuations in fluidized beds were identified by Lirag and Littman (1971) and Fan et al. (1981) from analyzing the recorded probability density function, auto-correlation function, and power spectral density function of the pressure fluc-

Correspondence concerning this article should be addressed to Y.-R. Yang.

tuations. Turner and Irving (1983) reported a well-defined pressure frequency for a bed height to width ratio greater than one, and they attributed this to slugging, with bursting slugs generating pressure waves which propagated down the bed. For aspects ration less than unity, "slugging ceases and the pressure waves within the bed become random." Fan et al. (1990) were the first to apply the concept of fractional Brownian motion (fBm) for analyzing pressure fluctuations in a gas-liquid-solid fluidized bed in terms of Hurst's rescaled range (R/S) analysis. The presence of one or more periodic components in pressure fluctuations was confirmed, because the presence of a break in every R/S curve was observed in the POX diagram. They concluded that the signals of pressure fluctuations are composed of a random component following fBm and one or more periodic components. He et al. (1997) demonstrated that the pressure fluctuations in a gas-solids fluidized bed can be decomposed into the addition of fBm and Gwn (Gaussian white noise). Stringer (1989) was the first to suggest that the gas-solid fluidized-bed's dynamic behavior might be interpreted as being chaotic. Since then, many studies have been carried out to characterize this dynamic behavior by means of chaos invariants such as correlation dimension, Lyapunov exponent, Kolmogorov entropy (Daw et al., 1990, 1995; van den Bleek and Schouten, 1993a,b; Bouillard and Miller, 1994; Hay et al., 1995; Cassanello et al., 1995; Schouten et al., 1996; Karamavruc and Clark, 1997; Marzocchella et al., 1997; Huilin et al., 1997; Bai et al., 1997; Schouten and van den Bleek, 1998; Zijerveld et al., 1998; Bai et al., 1999; Ji et al., 2000 and so on). One very important point in chaos theory is that the random-looking aperiodic behavior may be the product of determinism. This suggests that pressure fluctuations in fluidized beds would not stem from some stochastic process but some deterministic mechanism.

The definition of chaos includes three elements: determinism, aperiodicity, and sensitive dependence on initial conditions (Kaplan and Glass, 1995). A variety of invariants by analyzing pressure fluctuations have been proposed to characterize their complexity. For example, power spectra are particularly suitable for analysis of linear systems, where their interpretation is often transparent, whereas the dimension, Lyapunov exponent, and Kolmogorov entropy have been used to study geometrical and temporal properties of chaotic dynamics. However, none of these measures can be directly readily applied to determine if the dynamics to be studied are generated by a deterministic, rather than a stochastic, process (Kaplan and Glass, 1992). There has been a great interest in past years aimed at detecting "determinism" in time series. Three methods have been proposed as a clear hallmark of the existence of deterministic dynamic underlying a time series on the basis of different dynamical observations: continuity (Kaplan and Glass, 1992, 1993; Kaplan, 1994), smoothness (Ortega and Louis, 1998) and predictability (Kaplan and Glass, 1995; Salvino et al., 1995).

The objective of the present work is to develop a predictive model to detect determinism underlying pressure fluctuations and study predictability of pressure signals in a bubbling fluidized bed. The theory of phase-space reconstruction in deterministic chaos indicates that dynamic behavior of systems can be studied from the time evolution of any one observable variable, which is one of all variables describing the long-term evolution of a system, such as pressure fluctuations in fluidized beds. Based on this view, we present a discrete dynamic map equation showing trajectory evolution in reconstructed phase space and analyze rules of system evolution. The Jacobian matrix and any order of partial derivatives of this equation can be resolved at any time. The reliability of the model was testified.

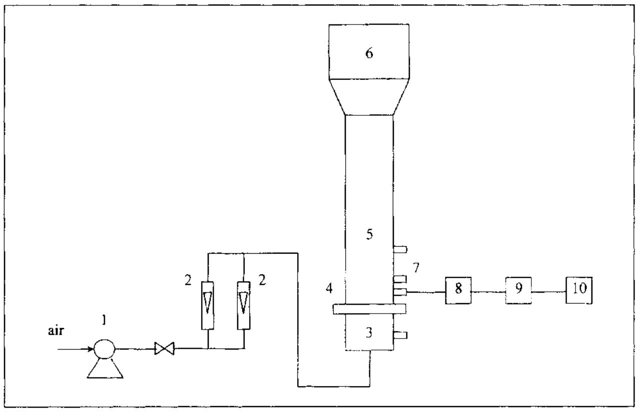

Figure 1. Experimental setup.

(1) Blower; (2) rotameter; (3) plenum; (4) distributor; (5) bed; (6) disengaging section; (7) pressure probes; (8) pressure transducers; (9) A/D board; (10) computer.

Experimental Studies

The experimental facilities are shown in Figure 1. The fluidized-bed assembly includes a bed column, a distributor, and a plenum chamber. The bed is 0.3 m in diameter and 3 m in height. The polyethylene (PE) particle was used as the fluidized particle; it has a density of 960 kg/m^3, and an average diameter of 500 μm. Its minimum fluidized-gas velocity u_{mf} is 0.118 m/s, and has a static-bed height of 0.46 m. The fluidizing fluid is air. The holes in the distributor were 2 mm in diameter and gave a fractional open area of 4%. Four piezoresistive pressure transducers (CYG219 type, Baoji Research Center of Transducer, China) were used to measure local pressure fluctuations. Pressure probes were installed on the wall of the bed column at four different heights from the distributor: 0.090 m, 0.20 m, 0.40 m above it, and 0.12 m below it, corresponding data run number C1, C2, C3, C4, respectively. Each pressure probe was connected to one of the two input channels of the differential pressure transducer, which produced an output voltage proportional to the pressure difference between the two channels. The remaining channel was exposed to the atmosphere. The differential range of the pressure transducer was $\pm$4kPa, and the relative accuracy was $\pm$0.1% full scale. The time series consisted of at least 60,000 points and were sampled at frequency 500 Hz using an analog-to-digital converter with 12 bit nominal resolution. A low-pass filtering at 20 Hz was always applied offline based on FFT before data analysis.

Predictive Model

The qualitative dynamic of a dissipative system may be inferred from an experimentally obtained time series of a variable that provides information on the whole system. The attractor that describes the evaluation of the system in state space may be reconstructed by generating vectors in an embedding state space from delayed measurements of one variable (Packard et al., 1980; Takens, 1981). For fluidizing systems, let us assume that the measured time series of pressure fluctuations is $p_1, p_2, \cdots, p_N$ and its sample interval is $\Delta t = 1/f_s$, we embedded it into R^m, Euclidean m-dimensional space, and got its subset, its element is

$$X_i(m,\tau) = (p_i, p_{i+\tau}, p_{i+2\tau}, \cdots, p_{i+(m-1)\tau}) \qquad i = 1,2,3, \cdots, N_m, \quad (1)$$

where $\tau = k\Delta t$ is delay time, $N_m = N-(m-1)\tau$ is the number of point in reconstructed pseudo-state-space. When these points

$$\begin{aligned} X_1 &= (p_1, p_{1+\tau}, p_{1+2\tau}, \cdots, p_{1+(m-1)\tau}) \\ X_2 &= (p_2, p_{2+\tau}, p_{2+2\tau}, \cdots, p_{2+(m-1)\tau}) \\ &\cdots \quad \cdots \quad \cdots \quad \cdots \quad \cdots \\ X_i &= (p_i, p_{i+\tau}, p_{i+2\tau}, \cdots, p_{i+(m-1)\tau}) \\ &\cdots \quad \cdots \quad \cdots \quad \cdots \quad \cdots \\ X_{N_m} &= (p_{N_m}, p_{N_m+\tau}, p_{N_m+2\tau}, \cdots, p_N) \end{aligned}$$

were connected, a trajectory which depicts dynamic behavior of system evaluation was obtained. Only if m and τ were chosen properly, set $\{X_i \in R^m\}$, which is a trajectory in reconstructed pseudo-state-space, is diffeomorphically equivalent to dynamic of real system.

We assume that the reconstructed fluidizing dynamic can be described using some deterministic map

$$X_{n+1} = F(X_n) \qquad (2)$$

where F: $R^m \to R^m$ is a map with $F = (f_1, f_2, \cdots, f_m)$ in reconstructed m-dimensional space. In fact, prediction of one point of the time series at next time P_{N+1} is prediction of one point in reconstructed m-dimensional space at next time X_{Nm+1}

$$X_{Nm+1} = (p_{Nm+1}, p_{Nm+1+\tau}, p_{Nm+1+2\tau}, \cdots, P_{N+1})^T$$

that is

$$\begin{cases} p_{Nm+1} = f_1(X_{Nm}) = f_1(p_{Nm}, p_{Nm+\tau}, p_{Nm+2\tau}, \cdots, p_N) \\ p_{Nm+1+\tau} = f_2(X_{Nm}) = f_2(p_{Nm}, p_{Nm+\tau}, p_{Nm+2\tau}, \cdots, p_N) \\ \cdots \quad \cdots \quad \cdots \quad \cdots \quad \cdots \\ P_{N+1} = f_m(X_{Nm}) = f_m(p_{Nm}, p_{Nm+\tau}, p_{Nm+2\tau}, \cdots, p_N) \end{cases} \qquad (3)$$

So, prediction of P_{N+1} can be realized by resolving the last term of Eq. 3. If X_{Kn} $(Kn < Nm)$ is the nearest neighbor to X_{Nm}, then

$$P_{N+1} = f_m(X_{Nm}) = f_m(X_{Kn} + X_{Nm} - X_{Kn}) \qquad (4)$$

Expanding the right of Eq. 4 in a Taylor series about the fiducial point X_{Kn}, we have

$$\begin{aligned} P_{N+1} = f_m(X_{Kn}) &+ \sum_{i=1}^{m} \frac{\partial f_m}{\partial x_i(Kn)}(x_i(Nm) - x_i(Kn)) \\ &+ \sum_{i=1}^{m}\sum_{j=1}^{m} \frac{\partial^2 f_m}{\partial x_i(Kn)\partial x_j(Kn)}(x_i(Nm) \\ &- x_i(Kn))(x_j(Nm) - x_j(Kn)) + \cdots \end{aligned} \qquad (5)$$

where $x_i(j) = p_{j+(i-1)\tau}$ and $f_m(X_{Kn}) = p_{Kn+1}$ can be measured by experiment, so Eq. 5 becomes the following

$$\begin{aligned} P_{N+1} &= p_{Kn+1} + Df_{m\beta}(x_\beta(Nm) - x_\beta(Kn)) \\ &+ D^2 f_{m\beta\zeta}(x_\beta(Nm) - x_\beta(Kn))(x_\zeta(Nm) - x_\zeta(Kn)) + \cdots \end{aligned} \qquad (6)$$

where

$$Df_{m\beta} = \frac{\partial f_m}{\partial x_\beta(Kn)}, \qquad D^2 f_{m\beta\zeta} = \frac{\partial^2 f_m}{2!\partial x_\beta(Kn)\partial x_\zeta(Kn)}, \quad \cdots \quad (\beta,\zeta = 1,2,\cdots,m) \qquad (7)$$

So, the question of prediction of P_{N+1} becomes how to resolve $Df_{m\beta}$, $D^2 f_{m\beta\zeta}$, $\cdots$ $(\beta,\zeta = 1,2,\cdots,m)$. Repeating the above process according to predictive P_{N+1}, the time series of pressure fluctuations can be predicted.

Computing $Df_{m\beta}$, $D^2 f_{m\beta\zeta}$, $\cdots$

Figure 2 shows the pseudo phase space construction of the pressure data using $\tau = 16\Delta t$ at $u = 0.314$ m/s. A trajectory of system evaluation with time $X_1, X_2, \cdots, X_{N_m}$ was obtained. If $X_n^r(0)$ is the rth nearest neighbor to X_n (neighbor was defined using Euclidean norm $n = 1, 2, \cdots, N_m$), then the displacement vector $Z_n^r(0)$ between $X_n^r(0)$ and X_n is shown as the following

$$Z_n^r(0) = X_n^r(0) - X_n \qquad (8)$$

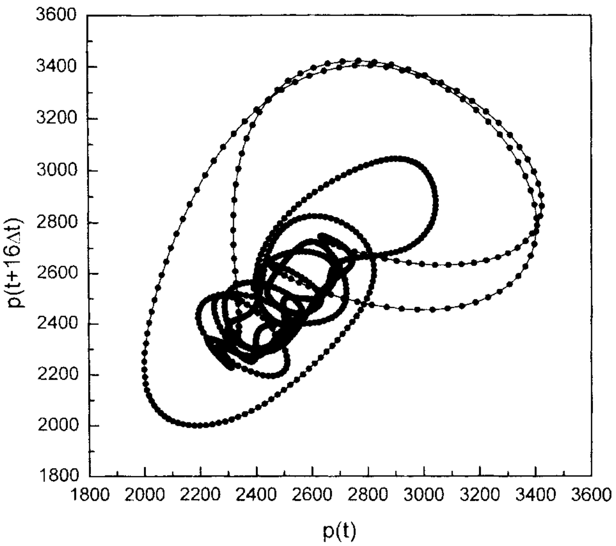

Figure 2. Reconstructed pseudo-phase space.

As shown in Figure 3, after the evolution of a time interval $T = k\Delta t$, the orbital point X_n will proceed to X_{n+T} and neighboring point $X_n^r(0)$ to $X_n^r(T)$. The displacement vector $Z_n^r(0)$ is thereby mapped to

$$Z_n^r(T) = X_n^r(T) - X_{n+T} = F(X_n^r(0)) - F(X_n) = F(X_n + Z_n^r(0)) - F(X_n) \quad (9)$$

Let $z_\alpha^r(n;k)$ be the αth component of $Z_n^r(k)$ ($\alpha = 1, 2, \cdots, m$). Then

$$z_\alpha^r(n;T_2) = f_\alpha(x_1(n) + z_1^r(n;0), x_2(n) + z_2^r(n;0), \cdots, x_m(n) + z_m^r(n;0)) - f_\alpha(x_1(n), x_2(n), \cdots, x_m(n)) \quad (10)$$

Similarly, expanding Eq. 10 in a Taylor series about the fiducial point X_n, we find

$$z_\alpha^r(n;T) = \sum_{i=1}^{m} \frac{\partial f_\alpha}{\partial x_i} z_i^r(n;0) + \frac{1}{2!} \sum_{i=1}^{m} \sum_{j=1}^{m} \frac{\partial^2 f_\alpha}{\partial x_i \partial x_j} z_i^r(n;0) z_j^r(n;0) + \cdots = Df_{\alpha\beta}(n) z_\beta^r(n;0) + D^2 f_{\alpha\beta\zeta}(n) z_\beta^r(n;0) z_\zeta^r(n;0) + \cdots \quad (11)$$

In practice, $Z_n^r(k)$ ($k = 1, 2, \cdots, N_m$) have been known from phase points in reconstructed pseudo-state-space. So Eq. 11 is a linear polynomial. At every fixed time, $Df_{\alpha\beta}$, $D^2 f_{\alpha\beta\zeta}$, $\cdots$ (α, $\beta, \zeta = 1, 2, \cdots, m$) can be obtained by a least-squares fit only if there are enough neighbors points Nb in reconstructed pseudo-state-space. It has been demonstrated by Briggs (1990) and Brown et al. (1991) that the total number of coefficients for different embedding dimension m and Taylor series of order NT is given by

$$Np = \left[\prod_{k=1}^{NT} \frac{m+k}{k} \right] - 1. \quad (12)$$

Thus, the minimum number of neighbors needed to give a unique solution of the least-squares problem is Np which grows rather rapidly with m and NT. (Using less than Np neighbors would result in an underdetermined least-squares fit.) We use at least twice this number of neighbors $Nb = 2Np$ in our least-squares fit of the residuals in Eq. 11. For different Taylor expanding series of order NT, we define matrices as the following

$$(V^\alpha)_{Nb \times 1} = \left[z_\alpha^1(n;T), z_\alpha^2(n;T), \cdots, z_\alpha^{Nb}(n;T) \right]^T$$

$$(B^\alpha)_{Np \times 1} = \left[Df_{\alpha 1}(n), Df_{\alpha 2}(n), \cdots, Df_{\alpha m}(n), D^2 f_{\alpha 11}(n), D^2 f\alpha_{12}(n), \cdots, D^2 F_{\alpha mm}(n), \cdots \right]^T$$

$$(Y)_{Nb \times Np} = \begin{bmatrix} z_1^1(n;0) & \cdots & z_m^1(n;0) & z_1^1(n;0) z_1^1(n;0) & z_1^1(n;0) z_2^1(n;0) & \cdots & z_m^1(n;0) z_m^1(n;0) & \cdots \\ z_1^2(n;0) & \cdots & z_m^2(n;0) & z_1^2(n;0) z_1^2(n;0) & z_1^2(n;0) z_2^2(n;0) & \cdots & z_m^2(n;0) z_m^2(n;0) & \cdots \\ \vdots & \cdots & \vdots & \vdots & \vdots & \cdots & \vdots & \cdots \\ z_1^{Nb}(n;0) & \cdots & z_m^{Nb}(n;0) & z_1^{Nb}(n;0) z_1^{Nb}(n;0) & z_1^{Nb}(n;0) z_2^{Nb}(n;0) & \cdots & z_m^{Nb}(n;0) z_m^{Nb}(n;0) & \cdots \end{bmatrix}$$

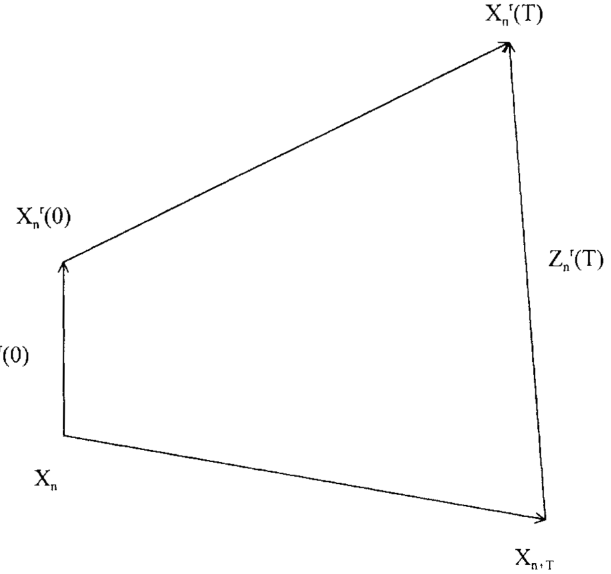

Figure 3. *r*th nearest neighbor to X_n and their evolvement.

So Eq. 11 can be changed as

$$V^\alpha = Y \cdot B^\alpha \qquad (\alpha = 1, 2, \cdots, m) \quad (13)$$

Then, the matrix B^α would be resolved using a least-squares algorithm for known matrices V^α and Y. We define

$$\phi = \| V^\alpha - Y \cdot B^\alpha \|^2. \quad (14)$$

The residual error shown as Eq. 14 would reach the minimum for obtaining the optimal estimation of B^α. For every element of B^α, B_i^α (that is $Df_{\alpha\beta}$, $D^2 f_{\alpha\beta\zeta}$, $\cdots$), we define

$$\frac{\partial \phi}{\partial B_i^\alpha} = 0 \qquad (i = 1, 2, \cdots, N_p) \quad (15)$$

then

$$B^\alpha = (Y^T \cdot Y)^{-1} \cdot Y^T \cdot V^\alpha. \quad (16)$$

So, B^α ($\alpha = 1, 2, \cdots, m$) would be obtained at any time. The predicted value of pressure signals p_{N+1} would be realized for reason that $Df_{\alpha\beta}$, $D^2f_{\alpha\beta\zeta}$, $\cdots$ (α, β, $\zeta = 1, 2, \cdots, m$) at any neighbor Kn showing as Eq. 6 can be obtained by Eq. 16.

However, there are two ways to do this. One is to use the model to predict the value at time $N+1$. Then we construct a new embedded point using this predicted value P_{N+1}

$$X_{Nm+1} = (p_{Nm+1}, p_{Nm+1+\tau}, p_{Nm+1+2\tau}, \cdots, P_{N+1})^T. \quad (17)$$

We then find the nearest points to X_{Nm-1} to make a prediction of the value at time $N+2$, which we call P_{N+2}. This process can be iterated, that is, we use past predictions to make future predictions. This method can in fact be used to extrapolate a time series beyond its measured values. The second way of making predictions, in order to predict the value at time $N+2$ is that we make the embedded point

$$X_{Nm-1} = (p_{Nm+1}, p_{Nm+1+\tau}, p_{Nm+1+2\tau}, \cdots, p_{N+1})^T. \quad (18)$$

Note that the measurement here is at time $N+1$, and not the prediction P_{N+1}; we are not using the past predictions to make future predictions.

Results and Discussion

Testing predictive model

To test the model presented above, capturing some important characteristics of the real system, we compared chaotic invariants of measured with model generated time series. We take the first half of the time series with 30,000 data points to construct a data-implicit model of the fluidizing dynamics. Then, we use the model to predict the values of the second half of the time series. For the purpose of testing the reliability of the predictive model it is better to use the first way to predict data, that is to generate a time series according to the past predictions to make future predictions. So, first of all, we must reconstruct dynamics from a scalar time series of pressure signals. However, to ensure that attractor in reconstructed pseudo-phase space is diffeomorphically equivalent to that in real phase space, it is very important to properly choose the embedding dimension m and time delay. According to Whitney's theorem, any smooth manifold of dimension d can be smoothly embedded in $m = 2d+1$ dimensions. In addition, Takens (1981) showed, with regard to reconstructions, that if the dimension of the manifold containing the underlying attractor is d, then embedding the data in a dimension $m \geq 2d+1$ preserves the topological properties of the attractor. More specifically, the embedding will be a diffeomorphism from the true phase space to the delay space. In our study, we found that pressure measurements showed the existence of a low order hydrodynamic attractor, whose dimension varied between 1.1 and 1.5 over the range of gas velocities studied by means of computing the correlation dimension using Grassberger-Procaccia's (1983b) algorithm. Similar results were demonstrated by Bouillard and Miller (1994). So embedding dimension $m = 4$ will be taken in the following study.

It is necessary to choose a proper time delay τ to reconstruct the phase space trajectories. It τ is too small, then the trajectories lie near the diagonal of the embedding space and, as τ is increased, the trajectories will expand from the diagonal so that they fill the complete m-dimensional phase space. Therefore, in the presence of experimental noise, the measured signal will be indistinguishable if small τ is used. On the other hand, large τ causes an uncorrelated time series in embedding space. Both causes make it difficult to characterize the attractor. Many criterions have been proposed to determine the time delay (see a review by Tsonis, 1992). Here, we especially pay close attention to the method of the mutual information function proposed by Fraser and Swinney (1986), because mutual information measures the general dependence of two variables regardless of linear or nonlinear. It is more appropriate than other methods such as the autocorrelation function when we are dealing with nonlinear dynamics. However, even so, there are some other cases reported by Daw and Halow (1993) and by Pence et al. (1995), where the first minimum of the mutual information function does not exist within any reasonable range. The same results were found from our experimental data. This makes it difficult to choose a qualitative time delay τ. Packard et al. (1980), Moon (1992), and Karamavruc et al. (1995) showed that the $x(t+\tau)$, which is the τ shifted version of measured signal $x(t)$, is related to $dx(t)/dt$. Both should have similar properties in phase plane. For example, a 2-D phase portrait can be constructed by plotting $x(t+\tau)$ against $x(t)$ which is called pseudo-phase space. This must be geometrically similar to the plots $dx(t)/dt$ vs. $x(t)$. So we choose time delay τ as embedding when a 2-D pseudo-phase portrait plotted by $p(t+\tau)$ against $p(t)$ is geometrically similar to the plots $dp(t)/dt$ vs. $p(t)$. As shown in Figure 4 the trajectories of (c) show more similarities to the phase-space trajectories constructed in (a) than the trajectories in (b) and (d). Therefore, the embedding time delay $\tau = 16\Delta t$ was taken.

The same method and process as above were used to determine the reconstructed parameters: the embedding dimension and the time delay at different gas velocities from different data run and the same results as in the following were obtained. But, to make things convenient for the following discussion, we only illustrate the results at $u = 0.408$ m/s

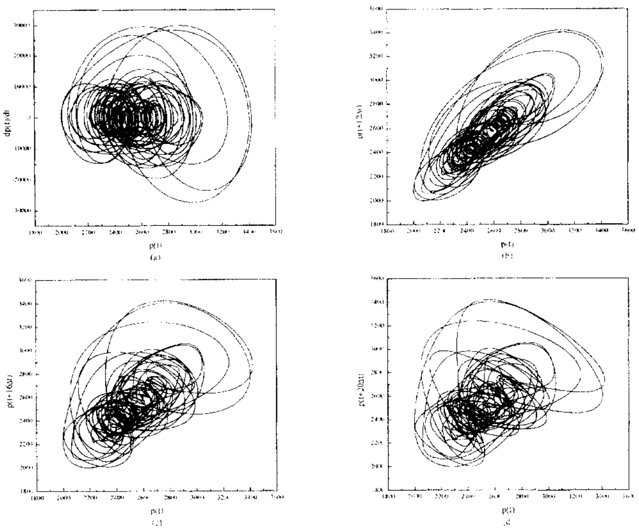

Figure 4. Phase space construction of pressure data at $u = 0.408$ m/s: (a) data run number C1; (b) pressure data using $\tau = 12\Delta t$; (c) $\tau = 16\Delta t$; (d) $\tau = 20\Delta t$.

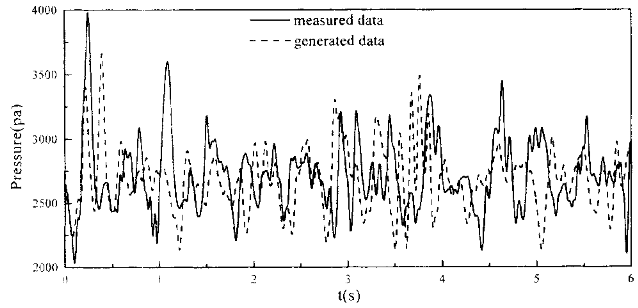

Figure 5. Measured vs. model generated time series of pressure signals.

from data run number C1 as an example. We take Taylor's expanding series of order as 2, comparison between measured and model generated time series of pressure signals were shown in Figure 5.

To test data generated by the model, if some important characteristics of the real system were retrieved, we computed chaotic invariants such as the correlation dimension, Kolmogorov entropy, and the spectrum of Lyapunov exponents from measured and model generated time series. Computation of the correlation dimension and Kolmogorov entropy proposed by Grassberger-Procaccia (1983a,b) is based on the correlation integral that is defined as

$$C_m(l) = \frac{1}{N(N-1)} \sum_{i \neq j} \Theta(l - \| X_i - X_j \|) \qquad (19)$$

where Θ is the Heaviside function defined as $\Theta(x) = 1$ for positive x and 0 otherwise, and l is the radius of a hypersphere centered on either the point i or j. The correlation exponent or dimension D_2 is a quantitative measure used for characterizing the local structure of an attractor. The estimation of D_2 can be determined from the relationship

$$C_m(l) \sim l^{D_2} 2^{-m\tau K_2} \qquad (20)$$

by plotting $\log_2 C_m(l)$ vs. $\log_2 l$ for values of m equal to 2 or greater. Each curve exhibits a region of linearity called as the no-scale interval, the slope of which corresponds to D_2. As the dimension m is increased beyond the embedding dimension, the linear region of the curves yield a consistent value of D_2 and are displaced from each other by a factor of $-m\tau K_2$. Here m represents the dimension in which the trajectories are embedded for evaluation of $C_m(l)$ and K_2 the order-2 Renyi Entropy. According to Eq. 20, an optimal algorithm for computing simultaneously the correlation dimension and K_2 entropy by a least-squares method was proposed by Zhao et al. (1999). K_2 of estimates obtained using this method is slightly lower than the actual values of the Kolmogorov entropy.

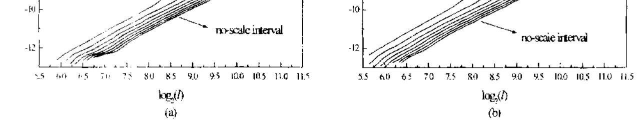

Figure 6. $\log_2 C_m^2(l) \sim \log_2 l$: (a) measured data; (b) generated data from model.

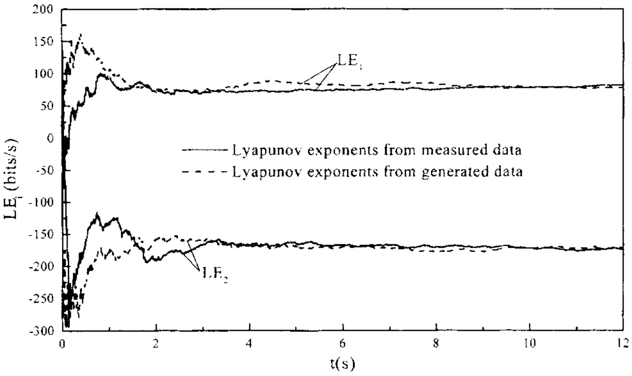

Figure 7. Convergence of Lyapunov exponents spectrum with time.

Figure 6 presents the relationship of $\log_2 C_m(l)$ vs. $\log_2 l$ from measured and model generated time series of pressure signals shown in Figure 5. The near similar correlation dimension and K_2 entropy were obtained. Similarly, the convergence of the spectrum of Lyapunov exponents with time from measured and generated data is shown in Figure 7 using the algorithm proposed by Brown et al. (1991). It is clear that similar results were obtained too.

Comparison between chaotic invariants (correlation dimension, K_2 entropy and the spectrum of Lyapunov exponents) of measured and model generated time series of pressure signals at u = 0.408 m/s from different data run numbers was shown in Table 1. It is further confirmed that the nearly consistent chaotic invariants were obtained from measured and generated data by model. Similar results have been obtained at different gas velocities and different data run numbers. These results may further indicate that the model presented above has captured some important characteristics of the real system. So, we can use this model to study the determinism and the predictability of system dynamics.

Determinism of system dynamics

We say that a system is determinism when future events are causally set by past events. Whether an underlying deterministic is presented can be decided from data. Use the data to construct a model of the dynamics, and then see whether the predictions made from this model are accurate. If the

Table 1. Chaos Characteristic Parameters: Measured vs. Model Generated Time Series

Data	D_2		K_2 [bits/s]		LE1 [bits/s]		LE2 [bits/s]	
Run	Meas.	Model	Meas.	Model	Meas.	Model	Meas.	Model
C1	1.27	1.27	1.24	1.29	80.91	77.46	−174.06	−171.45
C2	1.26	1.25	1.27	1.06	77.48	78.34	−169.34	−176.99
C3	1.26	1.23	0.860	0.875	82.24	79.12	−158.29	−145.87
C4	1.26	1.24	1.34	1.37	78.91	71.77	−149.27	−149.01

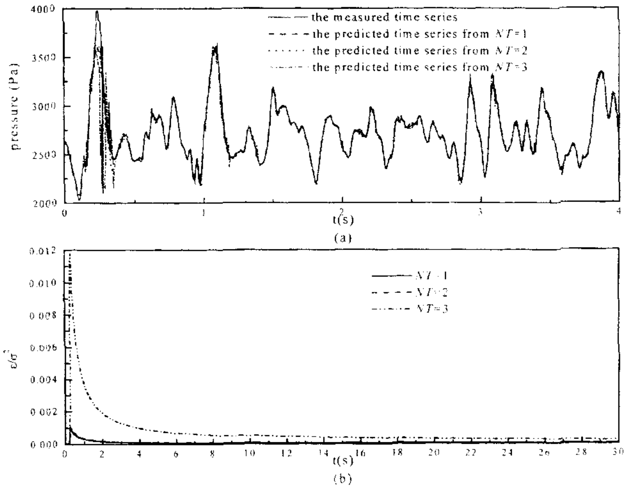

Figure 8. Diagnosis of determinism underlying pressure signals at $u = 0.408$ m/s from data run number C1.

(a) Measured time series and predicted time series for $NT = 1$, 2 and 3; (b) prediction error at different Taylor series.

predictions are perfect, then the system is completely deterministic. If the predictions are good, but not perfect, then the system has a deterministic component. If the predictions are terrible, then the system is not deterministic at all. We can construct a dynamical model from data as stated above because we have demonstrated that the predictive model proposed by us can capture some important nonlinear characteristics of real system.

As Kaplan and Glass (1995) suggested, to assess determinism in data, it is better to use the measured data directly to construct a new embedded point as showed in Eq. 18. That is, we are not using the past predictions to make future predictions. Given a predictive model for making a prediction P_{N+1}, we need to make an actual measurement of p_{N+1} in order to decide if the prediction is good or bad. The difference between P_{N+1} and p_{N+1} is the prediction error, which tells us about the quality of the prediction. Of course, a single prediction might be good or bad just by chance. To give a more meaningful indication of the determinism in the data, we can take the average of many prediction errors

$$\epsilon = \frac{1}{N} \sum_{k=1}^{N} (p_{N+k} - P_{N+k})^2. \tag{21}$$

Very large ϵ means the predictions are bad and the system is not deterministic. Conversely, small ϵ suggests that the system is deterministic. A convenient way to decide if ϵ is large or small is to compare it to the variance of the time series σ^2. We can do this by taking the ratio ϵ/σ^2, if this ratio is close to one, then the mean prediction error is large. If the ratio is close to zero, then the mean prediction error is small and the fluidizing system is deterministic. We define ϵ/σ^2 as the level of determinism of dynamics studied system.

Comparison between an actual value and a predicted value of pressure signal and their mean prediction error ϵ/σ^2 are shown in Figure 8 at $u = 0.408$ m/s from data run number C1 for different Taylor expanding series $NT = 1$, 2 and 3.

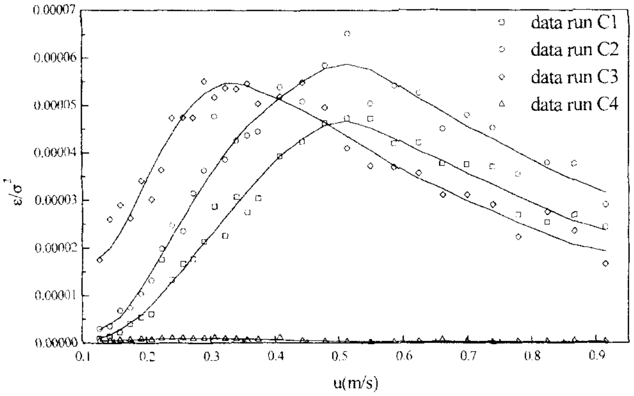

Figure 9. Mean prediction error ϵ/σ^2 at different gas velocities and different data run number for $NT = 1$.

The less prediction error at $NT = 1$ and 2 than $NT = 3$ is found. However, all the ratios ϵ/σ^2 are far away from unity and tend towards stability with time. The predictions are perfect, so we conclude that dynamics of the fluidizing system is completely deterministic.

The mean prediction error ϵ/σ^2 at different gas velocities and different data run number for $NT = 1$ is shown in Figure 9. Thus it is clear that the ratio ϵ/σ^2 is far less than unity over the range of gas velocities studied in the bubbling flow regime. Fluctuation dynamics studied the fluidizing system, which is further verified to be completely deterministic. It is therefore conjectured that some deterministic dynamics underlying pressure fluctuations surely exist. However, different tendencies of a deterministic level of system dynamics is found for different gas velocities and different data run corresponding to different measurement location distance from the distributor.

At low gas velocities, intermittent gas bubbles appeared to lead intermittent pressure fluctuations, therefore, the more deterministic dynamics and the quite small ϵ/σ^2 was observed. However, the waves of pressure would be attenuated at the process of propagation up to the surface of the bed and the deterministic level of dynamics would be declined. So, ϵ/σ^2 is decreased successively at location from the distributor 0.40 m, 0.20 m and 0.09 m at low gas velocities. With gas velocity increases, gas bubbles become gradually irregular and the deterministic level of system dynamics was reduced as ϵ/σ^2 increases. When stationary solid circulation patterns are formed at higher gas flows, deterministic levels of system dynamics begin to increase as ϵ/σ^2 decreases. So, there exists a maximum of ϵ/σ^2 for different location from the distributor with increases of gas velocities. However, a maximum of ϵ/σ^2 is reached earlier at location from distributor 0.40 m with gas velocity 0.335 m/s than with 0.20 m and 0.09 m with gas velocity 0.513 m/s. Experience suggests that three different zones can be distinguished within a bubbling bed: a distributor zone with vertical jets of gas or with very small bubbles, a bubbled bed, and a surface zone in which the bubbles burst throwing some particles into the freeboard. Locations from the 0.09 m and 0.20 m distributor lie in the zone of the bubbled bed and the location from the distributor 0.40 m lies in the surface zone. However, the bed expands gradu-

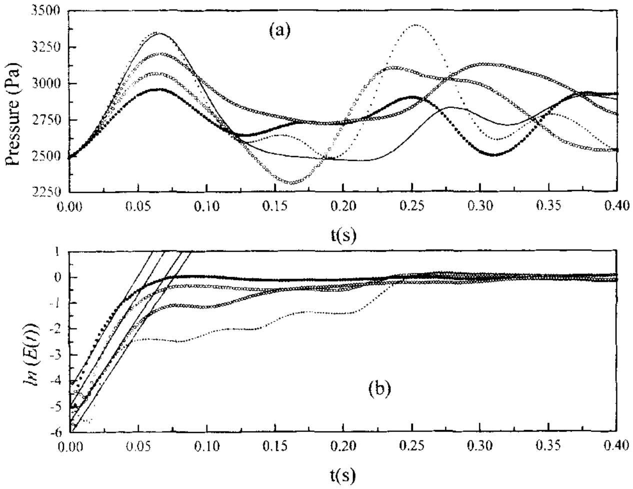

Figure 10. Long-term unpredictability of pressure fluctuations.

(a) Pressure fluctuations [measured —], [predicted, $NT = 1$ (○); $NT = 2$ (●); $NT = 3$ (◇); $NT = 4$ (+)]; (b) normalized root-mean-square error [$NT = 1$ (○), $NT = 2$ (●), $NT = 3$ (◇), $NT = 4$(+)].

ally with gas velocity increases, the mean bed height reaches 0.60 m when gas velocity reaches 0.335 m/s corresponding to the maximum of ϵ/σ^2. At this time, the point of pressure measurement distance from the 0.4 m distributor has become the zone of the bubbled bed and attenuation of pressure waves begin to decline. Thus, the deterministic level of system dynamics begins to gradually enhance at much higher gas velocities as ϵ/σ^2 decreases.

Since that one function of the distributor is to give a uniform distribution of gas across the bed, proper resistance between the distributor and bed is necessary. This makes many small fluctuations similar to random components to be attenuated in the plenum. So, the level of determinism or ϵ/σ^2 at location below the distributor 0.12 m is the minimum with respect to other locations above the distributor.

Long-term unpredictability of pressure fluctuations

Fluidizing systems obey certain deterministic rules that have been demonstrated as above for the fluidizing conditions studied. Table 1 shows that there exists a positive maximum in Lyapunov exponent spectrum. So the fluidizing system is a deterministic chaotic system. According to the chaos theorem, the system has limited predictive power because of their sensitivity to initial conditions and because we cannot make perfect measurements (which require an infinite amount of information). However, before their predictive power is lost (that is, for short time scales) their predictability may be quite adequate and possibly better than the predictive power of statistical forecasting. Figure 10 is one of our research results at gas velocity $u = 0.408$ m/s from data run number C1. Here we adapt the first way to predict, that is to say, we construct a new embedded point using previous predicted value. The prediction error E is the normalized root-mean-square error defined as

$$E = \sqrt{\epsilon} / \sigma. \tag{22}$$

Table 2. Slope of $\ln[E(t)] \sim t$ at Different Taylor Expanding Series

NT	1	2	3	4
K	81.07	81.51	77.90	80.54

As Figure 10 shows, different Taylor expanding series from 1 to 4 is used to predict pressure fluctuations. We find that the prediction error at $NT = 4$ is minimum. Also the relation between $\ln(E(t))$ and time t is linear at small time scales for different Taylor series. The results of linear regression between $\ln(E(t))$ and time t at small scales are shown in Table 2. It is clear that the slopes are nearly the same with the maximum of Lyapunov exponent for different Taylor series. So, the normalized root-mean-square error E may use the following equation to estimate

$$E \propto C \cdot e^{LE_1 \cdot t}. \tag{23}$$

It is very evident that the prediction errors of pressure fluctuations grow exponentially with time. Chaos in deterministic systems implies a sensitive dependence on initial conditions. This means that if two trajectories start close to one another in phase space, they will move exponentially away from each other for small times on the average. Any positive Lyapunov exponents that are the average exponential rate of divergence nearly orbit in phase space. Because experimental data inevitably contain external noise due to environmental fluctuations and limited experimental resolution, these deem that the long-term prediction of pressure fluctuations is impossible.

Conclusions

(1) A predictive model is presented to study predictability and determinism of dynamics underlying the pressure signals based on the measurement and analysis of the time series of the fluctuations of local pressure in a bubbling fluidized bed. Two methods are proposed to make predictions. One is to take the first half of the measured time series to construct a data-implicit model of the dynamics. Then, we use the model to predict the value at the next time $T+1$ is by constructing a new embedded point using the measured value at time T. This method can be used to study determinism of dynamics. The second method that we use with the model is to predict the value at the next time $T+1$ is by constructing a new embedded point using the predicted value at time T. This method can be used to study long-term predictability of dynamics.

(2) Comparison between chaotic invariants (correlation dimension, K_2 entropy, and the spectrum of Lyapunov exponents) of the measured and model generated time series of pressure signals shows that the model has captured some important nonlinear characteristics of the real system. So, we can use this model to study the determinism and the predictability of system dynamics.

(3) A new characteristic index ϵ/σ^2 defined as the level of determinism of dynamics is presented. Because ϵ/σ^2 is far less than unity over the range of gas velocities for different locations studied in the bubbling flow regime, it is verified that the fluctuation dynamics studied fluidizing system is completely deterministic. We can conjecture that some deter-

ministic dynamics underlying pressure fluctuations do exist. Different tendencies of deterministic levels of system dynamics are analyzed for different gas velocities and different data run corresponding to different measurement location distance from the distributor.

(4) The long-term unpredictability of pressure fluctuations is testified. The prediction errors of pressure fluctuations grow exponentially with time at short time scales and the rate of exponent separation between predicted values and measured values is proportional to the maximum of Lyapunov exponent.

Literature Cited

Bai, D., A. S. Issangya, and J. R. Grace, "Characteristic of Gas-Fluidized Beds in Different Flow Regimes," *Ind. Eng. Chem. Res.*, **38**, 803 (1999).

Bai, D., H. T. Bi, and J. R. Grace, "Chaotic Behavior of Fluidized Beds Based on Pressure and Voidage Fluctuations," *AIChE J.*, **43**, 1357 (1997).

Bi, H. T., J. R. Grace, and J. X. Zhu, "Propagation of Pressure Waves and Forced Oscillation of Fluidized Beds and their Effects on Measurements of Local Hydrodynamics," *Powder Technol.*, **82**, 239 (1995).

Bouillard, J. X., and A. L. Miller, "Experimental Investigations of Chaotic Hydrodynamic Attractors in Circulating Fluidized Beds," *Power Technol.* **79**, 211 (1994).

Brereton, C. M. H., and J. R. Grace, "The Transition to Turbulent Fluidization," *Trans. Inst. Chem. Eng.*, **70**, 246 (1992).

Briggs, K., "An Improved Method for Estimating Liapunov Exponents of Chaotic Time Series," *Phys. Lett. A*, **151**, (1,2) 27 (1990).

Brown, R., P. Bryant, and H. D. T. Abarbanel, "Comparing the Lyapunov Spectrum of a Dynamical System from an Observed Time Series," *Phys. Rev. A*, **43**, 2787 (1991).

Cassanello, M., F. Larachi, M. N. Marie, C. Guy, and J. Chaouki, "Experimental Characterization of the Solid Phase Chaotic Dynamics in Three-Phase Fluidization," *Ind. Eng. Chem. Res.*, **34**, 2971 (1995).

Daw, C. S., C. E. A. Finney, M. Vasudevan, N. A. Van Goor, K. Nguyer, D. D. Bruns, E. J. Kostelich, C. Grebogi, E. Ott, and J. A. Yorke, "Self Organization and Chaos in a Fluidized Bed," *Phys. Rev. Lett.*, **75**, 2308 (1995).

Daw, C. S., and J. S. Halow, "Evaluation and Control of Fluidization Quality through Chaotic Time Series Analysis of Pressure Drop Measurements," *AIChE Symp. Ser.*, **89** (296), 103 (1993).

Daw, C. S., W. F. Lawkins, D. J. Downing, and N. E. Clapp, Jr., "Chaotic Characteristics of a Complex Gas-Solid Flow," *Phys. Rev. A*, **41**, 1179 (1990).

Fan, L. T., D. Neogi, M. Yashima, and R. Nassar, "Stochastic Analysis of a Three-Phase Fluidized Bed: Fractal Approach," *AIChE J.*, **36**, 1529 (1990).

Fan, L. T., T. C. Ho, S. Hiraoka, and W. P. Walawender, "Pressure Fluctuation in a Fluidized Bed," *AIChE J.*, **27**, 388 (1981).

Fraser, A. M., and H. L. Swinney, "Independent Coordinates for Strange Attractors from Mutual Information," *Phys. Rev. A*, **33**(2), 1134 (1986).

Grassberger, P., and I. Procaccia, "Estimation of the Kolmogorov Entropy from a Chaotic Signal," *Phys. Rev. A*, **28**, 2591 (1983a).

Grassberger, P., and I. Procaccia, "Characterization of Strange Attractors," *Phys. Rev. Lett.*, **50**, 346 (1983b).

Hay, J. M., B. H. Nelson, C. L. Briens, and M. A. Bergougnon, "The Calculation of the Characteristics of a Chaotic Attractor in a Gas-Solid Fluidized Bed," *Chem. Eng. Sci.*, **50**, 373 (1995).

He, Z., W. Zhang, K. He, and B. Chen, "Modeling Pressure Fluctuations via Correlation Structure in a Gas-Solids Fluidized Bed," *AIChE J.*, **43**, 1919 (1997).

Huilin, L., D. Gidaspow, and J. X. Bouillard, "Dimension Measurements Hydrodynamic Attractors in Circulating Fluidized Beds," *Power Technol.*, **90**, 179 (1997).

Ji, H., H. Ohara, K. Kuramoto, A. Tsutsumi, K. Yoshida, and T. Hirama, "Nonlinear Dynamics of Gas-Solid Circulating Fluidized-Bed System," *Chem. Eng. Sci.*, **55**, 403 (2000).

Kaplan, D. T., "Exceptional Events as Evidence for Determinism," *Physica D*, **73**, 38 (1994).

Kaplan, D. T., and L. Glass, "Direct Test for Determinism in a Time Series," *Phys. Rev. Lett.*, **68**, 427 (1992).

Kaplan, D. T., and L. Glass, "Coarse-Grained Embedding of Time Series: Random Walks, Gaussian Random Processes, and Deterministic Chaos," *Physica D*, **64**, 431 (1993).

Kaplan, D., and L. Glass, *Understanding Nonlinear Dynamics*, Springer-Verlag, New York (1995).

Karamavruc, A. I., and N. N. Clark, "Local Differential Pressure Analysis in a Slugging Bed Using Deterministic Chaos Theory," *Chem. Eng. Sci.*, **52**, 357 (1997).

Karamavruc, A. I., N. N. Clark, and J. S. Halow, "Application of Mutual Information Theory to Fluid Bed Temperature and Differential Pressure Signal Analysis," *Powder Technol.*, **84**, 247 (1995).

Lee, G. S., and S. D. Kim, "Pressure Fluctuations in Turbulent Fluidized Beds," *J. Chem. Eng. Jpn.*, **21**, 515 (1988).

Lirag, R., and H. Littman, "Statistical Study of the Pressure Fluctuations in a Fluidized Bed," *AIChE Symp. Ser.*, **67**, 11 (1971).

Marzocchella, A., R. C. Zijerveld, J. C. Schouten, and C. M. van den Bleek, "Chaotic Behavior of Gas-Solids Flow in the Riser of a Laboratory-Scale Circulating Fluidized Bed," *AIChE J.*, **43**, 1458 (1997).

Moon, F. C., *Chaotic and Fractal Dynamics*, Wiley, New York (1992).

Ortega, G. J., and E. Louis, "Smoothness Implies Determinism in Time Series: A Measure Based Approach," *Phys. Rev. Lett.*, **81** (20), 4345 (1998).

Packard, N. H., J. P. Crutchfield, J. D. Farmer, and R. S. Shaw, "Geometry from a Time Series," *Phys. Rev. Lett.*, **45**, 712 (1980).

Pence, D. V., D. E. Beasley, and J. B. Riester, "Deterministic Chaotic Behavior of Heat Transfer in Gas Fluidized Beds," *J. Heat Transfer*, **117**, 465 (1995).

Salvino, L. W., R. Cawley, C. Grebogi, and J. A. Yorke, "Predictability in Time Series," *Phys. Lett. A*, **209**, 327 (1995).

Schouten, J. C., and C. M. van den Bleek, "Monitoring the Quality of Fluidization Using the Short-term Predictability of Pressure Fluctuations," *AIChE J.*, **44**, 48 (1998).

Schouten, J. C., M. L. M. van der Stappen, and C. M. van den Bleek, "Scale up of Chaotic Fluidized Bed Hydrodynamics," *Chem. Eng. Sci.*, **51**, 1991 (1996).

Stringer, J., "Is a Fluidized Bed a Chaotic Dynamics System," *Proc. 10th Int. Conf. on Fluidized Bed Combustion*, 265 (1989).

Takens, F., *Lecture Notes in Mathematics*, Springer, New York, **898**, 366 (1981).

Tsonis, A. A., *Chaos from Theory to Applications*, Plenum Press, New York (1992).

Turner, M. J., and D. Irving, "Forces on Tubes Immersed in a Fluidized Bed," *Proc. Int. Conf. on Fluidized Bed Combustion*, 831 (1983).

van den Bleek, C. M., and J. C. Schouten, "Can Deterministic Chaos Create Order in Fluidized Bed Scale-up," *Chem. Eng. Sci.*, **48**, 2367 (1993a).

van den Bleek, C. M., and J. C. Schouten, "Deterministic Chaos: a New Tool in Fluidized Bed Design and Operation," *Chem. Eng. J.*, **53**, 75 (1993b).

Van der Schaaf, J., J. C. Schouten, and C. M. van den Bleek, "Origin, Propagation and Attenuation of Pressure Waves in Gas-Solid Fluidized Beds," *Powder Technol.*, **95**, 220 (1998).

Verloop, J., and P. M. Heertjes, "Periodic Pressure Fluctuations in Fluidized Beds," *Chem. Eng. Sci.*, **29**, 1035 (1974).

Yerushalmi, J., and N. T. Cankurt, "Further Studies of the Regimes of Fluidization," *Powder Technol.*, **24**, 187 (1979).

Zhao, G. B., Y. F. Shi, W. F. Duan, and H. R. Yu, "Computing Fractal Dimension and the Kolmogorov Entropy from Chaotic Time Series," *Chinese J. Comput. Phys.*, **16**, 309 (1999).

Zijerveld, R. C., F. Johnsson, A. Marzocchella, J. C. Schouten, and C. M. van den Bleek, "Fluidization Regimes and Transitions from Fixed Bed to Dilute Transport Flow," *Powder Technol.*, **95**, 185 (1998).

Manuscript received Aug. 28, 2000.